CLM - P 535

CLM - P 535

UKAEA

Preprint

THE EFFECT OF SECONDARY ELECTRON EMISSION ON A PLASMA SHEATH

P J HARBOUR

CULHAM LABORATORY
Abingdon Oxfordshire

1978

CLM-P535

THE EFFECT OF SECONDARY ELECTRON EMISSION ON A PLASMA SHEATH

Peter J Harbour

Euratom-UKAEA Fusion Association, Culham Laboratory
Abingdon, OX14 3DB, England

Abstract

Sheath potential and heat transfer across the sheath have been studied for the case of a plasma in contact with a wall that emits secondary electrons. The solutions are valid for arbitrary magnitude and spread of ion velocities and whether or not the plasma is at floating potential. To allow for electron loss at the wall the electron velocities are expressed as truncated Maxwellian distribution functions and these lead to plasma conditions which allow greater electron emission and heat transfer rate and lower sheath potentials than have previously been reported.

(Submitted for publication in Physics of Fluids)

May 1978

I. INTRODUCTION

This paper presents a study of the influence of electron emission on a plasma sheath. The sheath could be that on the wall of an experimental fusion device or of a possible fusion reactor, and of particular interest is the sheath at the target of a tokamak divertor.[1] The contiguous plasma will be almost fully ionized with high temperature and low density, so ionization and other collision processes can be neglected in the immediate vicinity of the sheath. This collisionless plasma is lost at the wall so if it is to exist in a steady state it must be generated elsewhere. For example, in considering the exhaust flow along the magnetic field lines of a tokamak fusion reactor divertor, the main toroidal plasma within the separatrix may be considered to be an equilibrium source of plasma which flows collisionlessly through the divertor channel and thence through the target sheath to the wall[2]. Ions reaching the wall are assumed to recombine, moreover an equal global loss of electrons must also occur over the total area of the sheath although these losses need not balance locally.

The energy with which charged particles strike the wall can be high so both ions and electrons will yield appreciable numbers of secondary electrons. These secondary electrons are accelerated into the plasma by the electric field in the sheath. However, if the yield is so great that the resulting space-charge causes local electric field reversal at the wall, then some electrons are reflected back to the wall and the net electron emission current saturates at the space-charge-limited value. Secondary electron emission causes a reduction in sheath potential such that an additional current of electrons from the plasma can reach the wall.

The objectives of this paper are: (a) to determine the influence

of secondary electron emission on sheath potential; (b) to establish the limitations on sheath parameters when the emitted electron current saturates due to its space-charge and to find a Bohm stability criterion which takes the emitted electrons into account; (c) to derive an expression relating the energy transported by particles through the sheath to the sheath potential, which itself is a function of secondary electron yield; (d) to map the general regime of validity for the solutions obtained for potential, electron emission coefficient and heat transfer; and finally (e) although this paper deals predominently with a deuterium/tritium plasma (m_i is taken to be 2.5 amu) it is considered desirable to investigate how the results vary with ion mass.

It is necessary to consider the flux and energy carried by each specie, ions, thermal electrons and secondary electrons. It is convenient to evaluate the energy transfer at the wall rather than at the boundary between plasma and sheath, for then the energy transferred by emitted electrons is negligible and other simplifications can also be made. The model used is discussed in detail in Section II. It allows the ions to have a substantial drift velocity towards the wall such that they may be supersonic or subsonic with respect to the acoustic wave speed in the plasma and the energy transported by the ions is enhanced by the energy they gain in traversing the sheath. The thermal electrons in the collisionless plasma and in the sheath are not Maxwellian because, although they come from a collisional plasma at temperature T_e, the more energetic among them reach the wall and are assumed to be lost, so there is a deficiency of energetic electrons travelling away from the wall. The electron velocity

distribution function in the model is truncated to allow for this. The velocity distribution of the secondary electrons at any location in the sheath or collisionless plasma is a delta function about the velocity that they gain as a consequence of being accelerated from the wall. All of the electrons traversing the collisionless plasma in the direction away from the wall are assumed to come into equilibrium in the collisional region before returning. The analysis neglects the effect of magnetic fields.

To determine the limitations to sheath stability it is necessary to integrate the Poisson equation in the sheath. Apart from velocity distribution function instabilities which may be important but are beyond the scope of this paper there is the space-charge limit and also a Bohm-like stability criterion[3] for the velocity of plasma ions approaching the sheath. The latter must allow for the presence of secondary electrons. It will be shown that for a plasma with energetic ions this modified Bohm stability criterion is easily satisfied.

Previous studies of the influence of electron emission on a plasma sheath have been carried out by Hobbs & Wesson[4,5] but for plasmas containing low energy ions. The present study is different because it allows for more energetic ions with more general velocity distribution functions and more accurate electron distribution functions. Further, it does not require the assumption that the net current density of all charged particles to the wall must be zero at every point, even though it must be zero if integrated over the sheath on the whole of the plasma vessel.

II. DESCRIPTION OF THE PLASMA AND THE SHEATH

A parametric description of the plasma and sheath is now presented. This includes the spatial distribution of potential and current density of the various species together with the boundary conditions applicable on either side of the sheath. Once the velocity distribution functions of ions and electrons have been specified, then it is possible to write an expression for heat transfer through the sheath that is related to two parameters, namely the effective coefficient of secondary electron emission and the sheath potential. These two parameters are not independent and only when their relationship, which is discussed in Section III.1, has been determined can a complete expression for the heat transfer be deduced.

A. Description of the Potential, Current Density and Boundary Conditions

The sheath, the collisionless plasma and the thermalisation region are illustrated schematically in Fig.1, for a one-dimensional flow with constant area. The potential, V, is taken to be zero at the wall ($x = x_w$) and increases monotonically in the negative x-direction until at $x = 0$ the collisionless plasma is reached and the potential is assumed constant and equal to U thereafter. Fig.1(b) shows the non-dimensional version where

$$\phi = e(U-V)/kT_e \tag{1}$$

represents the potential whose value at the wall is

$$\phi_w = eU/kT_e \ . \tag{2}$$

The distance in non-dimensional form is

$$\xi = x/\lambda_D \tag{3}$$

where the Debye length

$$\lambda_D = (\varepsilon_o kT_e/n_o e^2)^{\frac{1}{2}} .$$

In the above equations n_o is the charged particle density at $x \leqslant 0$, T_e is the electron temperature in the thermalisation region and ε_o, k and e are, respectively, the permittivity of free space, Boltzmann's constant and the electronic charge.

The distribution of current density among the charged species is shown in Fig.1(c). The constant ion current density, j^+, throughout plasma and sheath is consistent with the assumed one-dimensional flow with the ions being lost at the wall. The secondary emission current density, j_s^-, is that released by incident ions and electrons subject to it not exceeding the space charge limited value. It is convenient to write $j^- + j_s^-$ for the thermal electron current density to the wall because $j^+ = j^-$ when the plasma is at floating potential. The boundary conditions on either side of the sheath are summarised in Table I.

Parameter		Collisionless Plasma	Wall
Distance	x	0	x_w
Normalised distance	ξ	0	ξ_w
Potential	V	U	0
Normalised potential	ϕ	0	ϕ_w
Normalised potential gradient	$\phi' = \frac{d\phi}{d\xi}$	0	ϕ'_w
Plasma density	n_i, n_e	$n_{io} = n_{eo} = n_o$	

Table I. Boundary conditions on either side of the sheath

B. The Velocity Distribution Functions

1. Distribution of ion velocities

In the collisionless plasma the distribution of ion velocities is assumed Maxwellian in the y and z directions but in the

x-direction it is truncated at $v_{ix} = 0$, thus if $0 \leqslant v_{ix} < \infty$, then

$$n_i(v_{ix}) = A_i \exp\left[- m_i(v_{ix} - u_i)^2/2kT_i\right], \qquad (4)$$

but $n_i(v_{ix})$ is zero for all negative values of v_{ix}. In Eq.4, A_i is the constant of normalisation, v_{ix} is the velocity of an ion in the x-direction, u_i is its most probable speed, T_i is the ion temperature characteristic of the collisionless plasma, m_i is the ion mass, and $n_i(v_{ix})d(v_{ix})$ is the ion density in the velocity range $\left[v_{ix}, v_{ix} + d(v_{ix})\right]$. This distribution function is illustrated in Fig.2(a). In practice such a simple expression may not be applicable but Eq.4 has the advantage of describing all types of ion flow from subsonic to supersonic with respect to the ion sound speed. The parameters used in Eq.4 can be made more convenient for the analysis in this paper, which uses non-dimensional equations, by the introduction of two non-dimensional parameters. The first is the ion speed ratio, s_i, which is the ratio of the most probable ion velocity in the x-direction to a typical thermal speed:

$$s_i = (\tfrac{1}{2} m_i u_i^2/kT_i)^{\frac{1}{2}} . \qquad (5)$$

The second parameter, called here the ion energy transport coefficient, δ_i, describes the magnitude of the ion energy. It is the average number of units of energy, kT_e, carried in the x-direction by each ion in the plasma and it can be shown[6] that $\delta_i kT_e$ may be expressed in terms of the ion temperature and speed ratio:

$$\delta_i kT_e = kT_i L(s_i), \qquad (6)$$

where

$$L(s_i) = \frac{(s_i^2 + 2)\exp(- s_i^2) + \sqrt{\pi}(s_i^2 + \frac{5}{2})s_i(1 + \operatorname{erf} s_i)}{\exp(- s_i^2) + \sqrt{\pi}\, s_i(1 + \operatorname{erf} s_i)}, \qquad (7)$$

with

$$\operatorname{erf} s_i = \frac{2}{\sqrt{\pi}} \int_0^{s_i} \exp(- \eta^2) d\eta .$$

Equation 7 is complex but L varies smoothly from 2 when $s_i = 0$ to s_i^2 when $s_i \to \infty$. Thus for a half range Maxwellian with $s_i = 0$, Eq.6 yields the standard kinetic theory result of 2 kT_i for the mean energy carried by an ion. At the other extreme for mono-energetic ions ($s_i \to \infty$) with velocity u_i, then the mean energy carried by each ion is $kT_i\, L(\infty)$ and becomes $kT_i s_i^2$, which, using Eq.5, is equal to $\frac{1}{2} m_i u_i^2$ as would be expected.

The analysis in this paper is valid for all values of s_i and δ_i, provided the Bohm limit ($\delta_i \gtrsim 0.5$) is satisfied. This is more general than the earlier work of Hobbs and Wesson[4,5] which was restricted to cold ion plasmas with δ_i barely satisfying the Bohm stability limit, and for analytical simplicity s_i was taken to be infinite. Despite this generality it has still been necessary in the present analysis to restrict some of the calculations to the case $s_i \to \infty$. Numerical evaluation has been performed for ion energies extending up to $\delta_i = 2.5$, which is unlikely to be exceeded in a streaming plasma. The reason why any particular values of s_i and δ_i should occur is beyond the scope of this work because they are related to processes in the thermalisation region[2]. If the collisionless plasma were in fact an ion beam, then δ_i would considerably exceed 2.5, nevertheless the analysis would still be applicable to such a plasma.

2. Distribution of electron velocities

In both plasma and sheath the thermal electron velocity distribution function (excluding secondary electrons) is assumed Maxwellian at temperature T_e in the y and z directions, while in the x-direction it is truncated such that,

$$n(v_{ex}) = A_e \exp\{ -[\tfrac{1}{2} m_e v_{ex}^2 + e(U-V)]/kT_e \}, \qquad (8)$$

in the range $-(2eV/m_e)^{\frac{1}{2}} \leq v_{ex} < \infty$, but $n(v_{ex})$ is zero if

$v_{ex} < -(2eV/m_e)^{\frac{1}{2}}$. Here A_e is the constant of normalisation and v_{ex} is the velocity of an electron in the x-direction.

This distribution function is illustrated in Fig.2(b) which also indicates a delta function for the secondary electrons. Electrons approaching the wall, ($v_{ex} \geq 0$) are characterised by a half range Maxwellian function so their mean thermal speed is unchanged by the sheath potential but their density, and therefore the flux towards the wall, is attenuated by the factor $\exp(eU/kT_e)$. As a consequence in the collisionless plasma the electron current density towards the wall, $(j^- + j_s^-) \exp(eU/kT_e)$ shown in Fig.1(c) includes this exponent. The corresponding current density in the reverse direction is the difference between the incident fluxes on the sheath at x = 0 and on the wall at $x = x_w$, also shown in Fig.1(c).

C. The Heat Transfer through the Sheath

The heat transfer to the wall is

$$\dot{q} = [j^+ E_{iw} + (j^- + j_s^-)E_{ew} - j_s^- E_{sw}]/e$$

where E_{iw}, E_{ew} and E_{sw} are respectively the mean energy transported at the wall by each ion, each thermal electron and each secondary electron. The ions gain energy eU in crossing the sheath so the energy they deposit on the wall is

$$E_{iw} = \delta_i kT_e + eU.$$

For electrons incident on the wall standard kinetic theory shows that

$$E_{ew} = 2\ kT_e.$$

Secondary electrons are emitted with insignificant energies so E_{sw} is negligible, and so if radiation is neglected the heat flux to the wall can be expressed as

$$\dot{q} = j^+(\delta_i kT_e/e + U) + (j^- + j_s^-)\ (2kT_e/e). \qquad (9)$$

To express the heat transferred by each ion and its associated thermal and secondary electrons, Eq.9 can be made non-dimensional to yield, in conjunction with Eq.2, an energy transport coefficient

$$\delta_t = \frac{\dot{q}e}{j^+ kT_e} = \delta_i + \phi_w + 2\left[\frac{j^-}{j^+} + \Gamma_s\right]. \qquad (10)$$

This approach has the advantage that it includes

$$\Gamma_s = j_s^-/j^+ \qquad (11)$$

which is an effective coefficient for secondary electron emission at the wall. This coefficient can be determined by writing the secondary electron current density at the wall

$$j_s^- = \gamma^+ j^+ + \gamma^- (j^- + j_s^-)$$

in terms of the secondary electron emission coefficients for impact by ions (γ^+) and electrons (γ^-), thus

$$\Gamma_s = [\gamma^+ + \gamma^-(j^-/j^+)]/(1 - \gamma^-). \qquad (12)$$

When γ^+ and γ^- are both small, Γ_s tends to zero and δ_t tends to a minimum value. Conversely when γ^- approaches unity, which is likely to occur for some practical conditions then the space charge of secondary electrons causes Γ_s to saturate as discussed in Section III.D.2.

III. RESULTS

A. Variation of Sheath Potential with Secondary Electron Yield

In the plasma the density of both thermal and secondary electrons is controlled by the sheath potential in such a manner that their combined density is equal to the ion density. Thus if these densities are known, the sheath potential can be determined.

The ion density in the collisionless plasma can be shown to be

$$n_{io} = \left(\frac{j^+}{e}\right) \left(\frac{\pi m_i}{\delta_i kT_e}\right)^{\frac{1}{2}} F(s_i), \qquad (13)$$

where

$$F(s_i) = \left[2L(s_i)\right]^{\frac{1}{2}} \left[\frac{\frac{1}{2} + \frac{1}{2}\,\mathrm{erf}\, s_i}{\exp(-s_i^2) + \sqrt{\pi}\, s_i\, (1 + \mathrm{erf}\, s_i)}\right], \qquad (14)$$

with $L(s_i)$ given by Eq.7. $F(s_i)$ is illustrated in Fig.3 and varies from $F(0) = 1$ to $F(\infty) = 1/\sqrt{2\pi}$, so it is slowly varying in s_i. Thus the ion density in the plasma, as given by Eq.13, is not strongly influenced by the spread of ion velocities.

The electron density in the collisionless plasma can be shown to be

$$n_{eo} = \left(\frac{j^- + j_s^-}{e}\right)\left(\frac{2\pi m_e}{kT_e}\right)^{\frac{1}{2}} \left[\frac{1}{2} + \frac{1}{2}\,\mathrm{erf}\left(\frac{eU}{kT_e}\right)^{\frac{1}{2}}\right] \exp\left(\frac{eU}{kT_e}\right) + (j_s^-/e)\sqrt{m_e/2eU}, \qquad (15)$$

where on the right-hand side the first term represents the density of thermal electrons obtained by integrating the electron velocity distribution function, Eq.8, over the whole of velocity space. The second term is the density of secondary electrons in the collisionless plasma region.

The relationship between the non-dimensional sheath potential and the effective coefficient for secondary electron emission can now be obtained by equating the ion and electron densities in Eqs.13 and 15. Thus

$$\left(\frac{2\pi}{\delta_i}\frac{m_i}{m_e}\right)^{\frac{1}{2}} F(s_i) = \left(\frac{j^-}{j^+} + \Gamma_s\right)\sqrt{\pi}\,(1 + \mathrm{erf}\,\sqrt{\phi_w})\,\exp\phi_w + \Gamma_s\,\phi_w^{-\frac{1}{2}}, \qquad (16)$$

where ϕ_w and Γ_s have been obtained from Eqs.2 and 11. Equation 16 is evaluated for Γ_s in terms of ϕ_w, m_i/m_e, δ_i and j^-/j^+. Figure 4 shows Γ_s plotted against ϕ_w for a range of values of δ_i ($0.498 \leq \delta_i \leq 2.5$). The plasma chosen for this evaluation is a deuterium/tritium mixture in which the ion mass is taken to be 2.5 amu. For simplicity a

floating potential sheath ($j^+ = j^-$) has been assumed and the ions incident upon the sheath are taken to be monoenergetic so $s_i \to \infty$. When secondary electron emission is negligible the non-dimensional sheath potential varies in response to variations in ion velocity which are implicit in the parameter δ_i, the potential being lowest for high δ_i which corresponds to low ion density. For substantial emission of secondary electrons characterised by $\Gamma_s \gtrsim 4$ the sheath potential drops to well below kT_e/e. In practice the yield of secondary electrons is determined by the physical properties of the wall material so the sheath potential is not an independent variable. In addition Γ_s is restricted by space charge saturation at the wall and the stability of the sheath is dependent upon a Bohm[3] criterion.

B. Limitation to Sheath Stability

1. Space charge limitation

When the secondary electron yield increases, the sheath potential decreases and so the emitted electrons are less strongly accelerated away from the wall and their density increases. This effect is most strongly evident near the wall because the secondary electron velocity is low and their density is correspondingly high. Conversely the ion density at this location is low because ions are accelerated towards the wall. The electric field at the wall is reduced because of the combined effect of high electron and low ion space charge. For higher electron yields the electric field at the wall becomes zero or even slightly negative but only sufficiently so to prevent further emitted electrons from traversing the sheath. The emitted electron current is space charge limited at this point. The conditions for space charge limitation in the sheath are derived in Sect.A of the Appendix and follow from the solution

of the Poisson equation which is also obtained in the Appendix. The algebra becomes rather complicated and so for simplicity the limiting solution has been found only for monoenergetic incident ions with an ion speed ratio $s_i \to \infty$. This means that the space charge limit and the modified Bohm limit (Section III.B.2) are derived only for monoenergetic ions. However, provided the electron emission is not space charge or Bohm limited, then the heat flux and potential solutions are still valid for arbitrary ion speed-ratio as well as for any value of Γ_s, m_i, j^+/j^- and δ_i.

The condition for space charge limitation may be expressed in terms of the normalised electric field, $\phi_w' = (d\phi/d\xi)_w$ at the wall which is derived in Sect.A of the Appendix. This non-dimensional field is

$$\phi_w'^2 = 4\delta_i\left[\left(1 + \frac{\phi_w}{\delta_i}\right)^{\frac{1}{2}} - 1\right] - \frac{2}{C_\infty}\frac{j^-}{j^+}\left(G - 2\sqrt{\phi_w} - \sqrt{\pi}\right)$$

$$- \frac{2(G - \sqrt{\pi})}{C_\infty}\,\frac{\left[C_\infty - (j^-/j^+)G\right]}{(G + \phi_w^{-\frac{1}{2}})} \qquad (17)$$

where $$G = G(\phi_w) = \sqrt{\pi}\,(1 + \operatorname{erf}\sqrt{\phi_w})\,\exp\phi_w \qquad (18)$$

and $$C_\infty = (\delta_i m_e/m_i)^{-\frac{1}{2}} \quad . \qquad (19)$$

The subscript ∞ is used because the derivation is only for $s_i \to \infty$. Thus the criterion for no space charge saturation of the emitted electron current dictates that ϕ_w be large enough to make the right-hand side of Eq.17 positive. The space charge limit is obtained by equating the right-hand side of (17) to zero and solving numerically. Such limits have been applied to the plasma data illustrated in Fig.4. The dashed curve represents the maximum in Γ_s and the corresponding minimum in sheath potential for a series of incident ion energies as represented by δ_i. The largest value

of Γ_s occurs for low incident ion energies and is just below 10, and here saturation occurs due to the large yield of secondary electrons. At higher incident ion energies the tendency to lower sheath potential results in lower acceleration of secondary electrons and to space charge saturation at small values of Γ_s.

2. The modified Bohm criterion

The sheath stability criterion derived by Bohm[3] is applicable to a sheath upon which monoenergetic ions are incident and within which there are Maxwellian electrons. Within the sheath the ion density decreases because the ions are accelerated towards the wall and the density of Maxwellian electrons decreases by the Boltzmann factor, $\exp(-\phi)$. It is essential to stability in the sheath that the ion density be always greater than the electron density and this is achieved[1] in the case of no secondary emission for the present notation if the ion energy transport coefficient, $\delta_i \gtrsim 0.5$. If this Bohm criterion is not satisfied then as ions enter the sheath their density falls more rapidly than does the electron density. As a result electric field reversal occurs at the sheath edge with ensuing instability.

When secondary electron emission is included and the electron velocities are expressed by the truncated distribution function discussed in Sect.II.B.2, then it is still possible to obtain the appropriate criterion for sheath stability by the methods used by Bohm[3] and by Hobbs and Wesson[4,5]. Firstly the non-dimensional electric field in the sheath is derived, as in Sect.B of the Appendix as a series expansion in ϕ (Eq.A13):

$$\phi'^2 = \left\{\left(1 - \frac{1}{2\delta_i}\right) - \Gamma_s\left(\frac{\delta_i}{\phi_w}\frac{m_e}{m_i}\right)^{\frac{1}{2}}\left[\frac{1}{2\phi_w} - \frac{j^-/j^+}{\Gamma_s}\right]\right\}\phi^2 + O(\phi^3). \qquad (20)$$

The modified Bohm criterion is now obtained by making the right-hand

side of Eq.20 positive for all values of ϕ. This is most critical when ϕ is small so the criterion is:

$$1 - \frac{1}{2\delta_i} \geq \Gamma_s \left(\frac{\delta_i}{\phi_w}\frac{m_e}{m_i}\right)^{\frac{1}{2}} \left[\frac{1}{2\phi_w} - \frac{j^-/j^+}{\Gamma_s}\right] \qquad (21)$$

or, if Γ_s is eliminated using Eq.16 and substituting from Eqs.18 and 19,

$$1 - \frac{1}{2\delta_i} \geq \frac{1 - (j^-/j^+)G/C_\infty}{1 + G\sqrt{\phi_w}} \left(\frac{1}{2\phi_w}\right) - \frac{j^-/j^+}{C_\infty \phi_w^{\frac{1}{2}}} . \qquad (22)$$

It is seen from Eq.21 that if $\Gamma_s = 0$ the criterion is that $\delta_i \geq 0.497$ for the plasma conditions of the D-T mixture illustrated in Fig.4. This is almost equivalent to the Bohm value of 0.5. The very small difference is due to the second term in the square brackets of Eq.21 and this is associated with the truncated Maxwellian electron distribution function, which was not featured in Bohm's derivation. For finite secondary emission ($\Gamma_s > 0$), the ion energy must be increased in order to continue to satisfy the inequality (21). The right-hand side is never large so a small increase in δ_i meets this requirement. The values of δ_i were obtained by a simple graphical solution of inequality (22) and some are shown in Fig.4. When δ_i exceeds 0.53 the Bohm criterion is easily satisfied and the space charge limit on the sheath stability becomes dominant.

C. Relationship between Heat Transfer and Sheath Potential

The heat transferred through the sheath by ions and all their associated electrons is characterised by the total energy transport coefficient δ_t. This is expressed in Eq.10 in terms of both Γ_s and ϕ_w. However, Γ_s can be eliminated using Eq.16, thus the heat transfer may be expressed explicitly in terms of sheath potential:

$$\delta_t = \delta_i + \phi_w + 2\left[C + (j^-/j^+)\phi_w^{-\frac{1}{2}}\right]/(G + \phi_w^{-\frac{1}{2}}) \qquad (23)$$

where

$$C = \left(\frac{2\pi}{\delta_i}\frac{m_i}{m_e}\right)^{\frac{1}{2}} F(s_i) \qquad (24)$$

and is related to C_∞ given in Eq.19.

The expression for δ_t given in Eq.23 is valid for any values of s_i, δ_i, ϕ_w and m_i provided that the Bohm and space charge saturation criteria for sheath stability are satisfied. Figure 5 shows the relationship between δ_t and sheath potential for a deuterium-tritium plasma sheath under the same conditions as are illustrated in Fig.4. Regardless of the value of δ_i, the lowest heat transfer occurs at the highest sheath potential which corresponds to no emission of secondary electrons from the wall. Under this condition the energy transported by each ion pair reaching the wall varies from 6 to 7 kT_e. This corresponds to 2 kT_e for the electrons and 4 to 5 kT_e for the ions, most of the ion energy being gained in the sheath. If the secondary electron emission is finite the extra electrons cause the plasma potential to decrease. Then more plasma electrons can reach the wall and heat transfer by electrons is increased. The ions gain less energy by acceleration through the reduced sheath potential so their heat transfer is reduced. However, the total heat transfer increases because it is now dominated by the contribution due to increased electron flux. Space charge and Bohm limits still apply so the shape of the limiting curves for heat transfer (δ_t in Fig.5) closely parallel those for the effective coefficient for secondary electron emission (Γ_s in Fig.4).

The maximum heat transfer ($\delta_t = 23$) occurs when $\delta_i = 0.53$ and $\phi_w = 0.87$. Thus the heat transfer is almost four times greater than that when no secondary electrons are emitted.

D. General Regime of Validity

Both space charge saturation and the Bohm criterion limit the maximum possible effective coefficient of secondary electron emission and therefore the minimum possible sheath potential. However, a further restriction to sheath potential leads to a maximum in ϕ_w when the secondary electron yield is zero. This may be obtained from Eq.16:

$$\left(\frac{2\pi}{\delta_i}\frac{m_i}{m_e}\right)^{\frac{1}{2}} F(s_i) = \frac{j^-}{j^+}\sqrt{\pi}\,(1 + \text{erf}\,\sqrt{\phi_w})\exp\phi_w \,. \qquad (25)$$

These three constraints imply that heat transfer through the sheath is also subject to restrictions.

1. Bounds to sheath potential

The range of possible floating sheath potentials has been plotted in Fig.6 as a function of the ion energy transport coefficient, δ_i, for the simplest case, namely monoenergetic ions ($s_i = \infty$). The plasma is again a deuterium-tritium mixture (m_i = 2.5 amu). The upper bound to sheath potential occurs when there is no secondary emission and is shown by the parameter $[\phi_w]_{\Gamma_s=0}$. This bound decreases when ion energy, characterised by δ_i, increases because then the ion density decreases and the plasma becomes more negative. The lower bound to sheath potential is determined firstly by space charge saturation $[\phi_w]_{sat}$ and is found by equating the right-hand side of Eq.17 to zero and solving numerically. This is also shown in Fig.6, it decreases with increasing δ_i in a comparable manner to $[\phi_w]_{\Gamma_s=0}$, differences in shape being associated with the influence of ion space charge on the saturation current of secondary electrons. The second lower bound to sheath potential is the modified Bohm criterion, $[\phi_w]_B$, which is conveniently obtained by equating the inequality (22). As can be seen from Fig.6 this bound is only important in the range

$0.497 \leqslant \delta_i \leqslant 0.53$. It is more effective as a lower bound for δ_i rather than for ϕ_w and in this region it is not very different from the classical Bohm limit, $\delta_i \geqslant 0.5$. If the plasma contains cold ions such that δ_i lies below this bound then, following Bohm, it would be expected that δ_i would be raised by instabilities. Hobbs and Wesson[4,5] have extended this concept to include secondary emission and argue that instabilities would cause $[\phi_w]_{sat} = [\phi_w]_B$. Under these conditions, shown by the point SB in Fig.6, the present analysis yields $[\delta_i]_{SB}=0.53$ and $[\phi_w]_{SB}=0.865$ for $m_i=2.5$ amu.

In order to compare the present analysis with that of Hobbs and Wesson, $[\phi_w]_{sat}$ has been determined for a Maxwellian electron distribution function and a floating potential sheath. This appears in Fig.6 as $[\phi_w]^{HW}_{sat}$ and has been obtained from the equation corresponding to (17) which is

$$\phi_w'^2 = 4\delta_i\left[\left(1 + \frac{\phi_w}{\delta_i}\right)^{\frac{1}{2}} - 1\right]$$

$$- \left\{4\,\frac{\sqrt{\pi}\left[\exp(\phi_w) - 1\right] + \phi_w^{\frac{1}{2}} + \left[(\pi/\phi_w)^{\frac{1}{2}}/C_\infty\right]\left[\exp(\phi_w)\,(2\phi_w - 1) - 1\right]}{2\sqrt{\pi}\,\exp(\phi_w) + \phi_w^{-\frac{1}{2}}}\right\}. \quad (26)$$

It is evident that the assumption of Maxwellian electrons raises the magnitude of the lower bound in sheath potential without significantly affecting its dependence on δ_i.

The correspondingly derived Bohm criterion, $[\phi_w]^{HW}_B$, is related to the inequality (21) and is:

$$1 - \frac{1}{2\delta_i} \geqslant \Gamma_s\left(\frac{\delta_i}{\phi_w}\frac{m_e}{m_i}\right)^{\frac{1}{2}}\left(\frac{1}{2\phi_w} + 1\right). \quad (27)$$

This bound is similarly raised and in both cases the increases arise because the neglect of truncation to the thermal electron distribution function leads to too many thermal and therefore too few secondary electrons. For a cold ion plasma the assumption

that instabilities increase δ_i until $[\phi_w]^{HW}_{sat} = [\phi_w]^{HW}_B$, yields $\delta_i = 0.58$, $\phi_w = 1$ for $m_i = 2.5$ amu. These correspond to the values quoted by Hobbs and Wesson[4,5] and the main difference is that the present analysis predicts lower values of sheath potential.

2. Bounds to electron emission coefficient

The bounds to Γ_s can be determined from the bounds to ϕ_w, which have been obtained for the simplest case ($s_i = \infty$). Substitution in Eq.16 leads to the corresponding parameters, $[\Gamma_s]_{sat}$ and $[\Gamma_s]_B$, which are shown in Fig.7, where Γ_s is plotted as a function of ion energy transport coefficient, δ_i. These bounds reflect the characteristics of the corresponding bounds to sheath potential. The parameters with superscripts, HW, have been obtained without truncation of the velocity distribution functions and so are equivalent to the Hobbs and Wesson approach. The magnitude of the upper bound to Γ_s is substantial and exceeds the Hobbs and Wesson prediction by 20%. In most practical cases the limit to secondary electron emission will be set by the surface properties of the wall. Because of the shapes of the curves of $[\Gamma_s]_{sat}$ and $[\Gamma_s]_B$ the maximum value of Γ_s lies close to its value $[\Gamma_s]_{SB}$ at the intersection point, SB, of these curves.

3. Bounds to heat transfer

The limitations to heat transfer can be similarly determined by substituting the limiting values to ϕ_w in Eq.23. These limits, $[\delta_t]_{sat}$, $[\delta_t]_B$ and $[\delta_t]_{\Gamma_s=0}$ are plotted in Fig.8 as a function of δ_i. The upper bound $[\delta_t]_{sat}$ is substantially greater than the value of 6 to 7 which would occur in the absence of secondary electron emission. The limits corresponding to the Hobbs and Wesson approach, $[\delta_t]^{HW}_{sat}$ and $[\delta_t]^{HW}_B$, restrict heat transfer through a stable sheath by up to 16%.

E. Influence of Ion Mass

Since the work described in this paper originated from a thermonuclear fusion study, most of the data have been evaluated for m_i = 2.5 amu. The equations are valid for any mass of ion but it was not intended here to provide a complete evaluation for every possible combination of mass, speed ratio and current density ratio, j^+/j^-. In this section a few results for different ion masses are gathered together.

When the electron emission is saturated the effect of ion mass upon the sheath potential, $[\phi_w]_{sat}$, can be determined from Eq.17 and is shown as a function of δ_i in Fig.9. The effect on the sheath potential at the modified Bohm limit $[\phi_w]_B$, determined from the inequality (21), is plotted as a function of δ_i in Fig.10. It is evident that ion mass does not significantly influence the sheath potential under these limiting conditions. Under conditions of saturated emission the lowest ion energies, characterised by $[\delta_i]_{SB}$, which satisfy the Bohm criterion $[\phi_w]_{sat} = [\phi_w]_B$ (see Sect. III.D.1 and Refs.4 & 5), are listed in Table II together with the corresponding values of $[\phi_w]_{SB}$. Although ion mass has a small effect upon the latter parameter, its effect upon $[\delta_i]_{SB}$ is negligible.

Also shown in Table II are the corresponding values $[\Gamma_s]_{SB}$ and $[\delta_t]_{SB}$ which to a first order are proportional to $m_i^{\frac{1}{2}}$.

Ion Mass, m_i (amu)	1	2.5	200
Ion energy transport coefficient, $[\delta_i]_{SB}$	0.525	0.53	0.532
Normalised sheath potential, $[\phi_w]_{SB}$	0.85	0.865	0.91
Max.effective secondary emission coeff.$[\Gamma_s]_{SB}$	6.01	9.78	90.44
Max. total energy transfer coeff., $[\delta_t]_{SB}$	15.39	22.96	184.3

Table II. The influence of ion mass on sheath parameters under the condition SB where the saturated emission and Bohm limits coincide. (The ion speed ratio $s_i \to \infty$ and the sheath is floating, $j^+/j^- = 1$)

For electron emission which is not saturated the influence of ion mass on the relationship between sheath potential and Γ_s can be determined from Eq.16. The ratio m_i/δ_i is an invariant in this equation so the analysis expressed in terms of δ_i (and shown in Fig.4) is applicable to the equivalent analysis in terms of m_i. As an example the curve showing $\delta_i = 2.5$ for a D-T plasma with $m_i = 2.5$ amu is applicable to a hydrogen plasma with $m_i = 1$ at $\delta_i = 1$. The corresponding effect of ion mass on heat transfer can be determined from Eq.23. Unfortunately the concept of invariance in m_i/δ_i can only be applied approximately to this equation. Quantitative determination of the effect must therefore be obtained by direct calculation. However, a qualitative indication can be obtained by applying the analogous argument of invariance to the data shown in Fig.5.

IV. CONCLUSION

The solutions for potential (16) and heat transfer (23) are valid for arbitrary incident ion energy and ion speed ratio, and whether or not the plasma is at floating potential. However the plasma stability, under conditions of the velocity distribution functions generated in this problem, has not yet been investigated, but the instabilities of such velocity distribution functions are well known. It may well be that these plasma instabilities restrict the regime of validity of the present analysis and the problem merits further consideration. For simplicity the determination of the regime of validity has only been carried out for monoenergetic incident ions, because the mathematical complexity for other ion speed ratios is considerable. However, the case of thermal ions ($s_i = 0$) should be relatively easy to evaluate.

No account has been taken in the present study of the influence of

magnetic fields on the sheath. In thermonuclear fusion applications very strong magnetic fields are present. Nevertheless the analysis should not be significantly affected by a magnetic field provided it is reasonably uniform and perpendicular to the sheath. For non-uniform fields the influence of the loss cone of magnetic mirrors should be taken into account in assessing the electron transport, while for non-perpendicular magnetic fields it is necessary to account for some suppression by the field of a proportion of the secondary electrons.

The present analysis indicates that the high electron temperatures which are anticipated in nuclear fusion devices might lead to sheath potentials of a kilovolt or more[1,2]. These high sheath potentials are likely to lead to unipolar arcing[7] and a study of such arcing, its avoidance and consequences, will be required before the results of this paper can be applied to very high temperature plasma sheaths.

ACKNOWLEDGMENT

The author thanks M F A Harrison whose comments and criticism have been much appreciated.

APPENDIX

The Solution of the Poisson Equation in the Sheath

For simplicity the sheath equations are solved for monoenergetic incident ions ($s_i = \infty$) so Eq.13 is rewritten, following the notation and equation numbers of the main text, in terms of n_o, the density of electrons or ions in the plasma,

$$n_o = \left(\frac{j^+}{e}\right) \left(\frac{m_i}{2\delta_i kT_e}\right)^{\frac{1}{2}} . \tag{A1}$$

The ion density in the sheath is obtained from continuity of j^+ and the ion energy, thus

$$n_i = n_o\left[1 + \frac{2e(U-V)}{m_i u_o^2}\right]^{-\frac{1}{2}} \tag{A2}$$

where u_o is the velocity of ions incident on the sheath.

The electron density in the sheath is obtained by rewriting Eq.15 of Sect.III.A with U replaced by V:

$$n_e = \left(\frac{j^- + j_s^-}{e}\right)\left(\frac{2\pi m_e}{kT_e}\right)^{\frac{1}{2}}\left[\tfrac{1}{2} + \tfrac{1}{2}\,\mathrm{erf}\left(\frac{eV}{kT_e}\right)^{\frac{1}{2}}\right]\exp\left(\frac{eV}{kT_e}\right)$$

$$+ (j_s^-/e)\sqrt{m_e/2eV} . \tag{A3}$$

The Poisson equation,

$$d^2V/dx^2 = e(n_e - n_i)/\varepsilon_o$$

where ε_o is the permittivity of free space, is written

$$\frac{d^2\phi}{d\xi^2} = \frac{n_i - n_e}{n_o} \tag{A4}$$

in non-dimensional form, where ϕ, ξ and λ_D are given by Eqs.1-3. By substituting from Eqs.1, 5, 6 and 7, Eq.A2 can be rewritten in non-dimensional form:

$$n_i/n_o = (1 + \phi/\delta_i)^{-\frac{1}{2}} . \tag{A5}$$

Also if Eqs.1, 2, 11 and A1 are substituted into Eq.A3, then it may

be rewritten in non-dimensional form:

$$\frac{n_e}{n_o} = \left(\frac{j^-}{j^+} + \Gamma_s\right) \left(\pi\, \delta_i \frac{m_e}{m_i}\right)^{\frac{1}{2}} \left[1 + \mathrm{erf}(\phi_w - \phi)^{\frac{1}{2}}\right] \exp(\phi_w - \phi)$$

$$+ \Gamma_s \sqrt{\frac{m_e}{m_i} \frac{\delta_i}{(\phi_w - \phi)}} \quad . \tag{A6}$$

Now Eq.A4 may be rewritten by substituting for n_i/n_o and n_e/n_o from Eqs.A5 and A6:

$$\phi'' = (1 + \frac{\phi}{\delta_i})^{-\frac{1}{2}}$$

$$- \left(\frac{j^-}{j^+} + \Gamma_s\right) \left(\pi\delta_i \frac{m_e}{m_i}\right)^{\frac{1}{2}} \left[1 + \mathrm{erf}(\phi_w - \phi)^{\frac{1}{2}}\right] \exp(\phi_w - \phi) - \Gamma_s \left[\frac{m_e}{m_i} \frac{\delta_i}{(\phi_w - \phi)}\right]^{\frac{1}{2}}, \tag{A7}$$

where the prime denotes $d/d\xi$.

Equation A7 can be integrated once by multiplying both sides by $2\phi'$:

$$2\int_0^{\xi} \phi'\phi''d\xi_1 = \int_0^{\xi} \frac{2\phi' d\xi_1}{(1+\frac{\phi}{\delta_i})^{\frac{1}{2}}}$$

$$- \left(\frac{j^-}{j^+} + \Gamma_s\right) \left(\pi\delta_i \frac{m_e}{m_i}\right)^{\frac{1}{2}} \int_0^{\xi} \left[1 + \mathrm{erf}(\phi_w - \phi)^{\frac{1}{2}}\right] \exp(\phi_w - \phi)\ 2\phi' d\xi_1$$

$$- \Gamma_s \left(\frac{m_e}{m_i}\delta_i\right)^{\frac{1}{2}} \int_0^{\xi} \frac{2\phi' d\xi_1}{(\phi_w - \phi)^{\frac{1}{2}}}$$

where ξ_1 is a dummy variable within the limits of integration given by $\xi_1 = 0$, $\xi_1 = \xi$. The lower limit $\xi_1 = 0$ corresponds to the boundary of the sheath with the collisionless plasma and here (from Table I) $\phi = 0$ and $\phi' = 0$ so the integrals yield the following expression for the electric field in the sheath:

$$\phi'^2 = 4\delta_i\left[(1+\frac{\phi}{\delta_i})^{\frac{1}{2}} - 1\right]$$

$$- 2\left(\frac{j^-}{j^+} + \Gamma_s\right) \left(\pi\delta_i \frac{m_e}{m_i}\right)^{\frac{1}{2}} \left[\exp \phi_w - \exp(\phi_w - \phi) + E(\phi_w) - E(\phi_w - \phi)\right]$$

$$- 4\Gamma_s \left(\frac{m_e}{m_i}\delta_i\right)^{\frac{1}{2}} \left[\phi_w^{\frac{1}{2}} - (\phi_w - \phi)^{\frac{1}{2}}\right] \tag{A8}$$

where $E(t) = \int_0^t \text{erf}\sqrt{u}\, du = \exp(t)\ \text{erf}\sqrt{t} - (2/\sqrt{\pi})\sqrt{t}$.

A second integration to find ϕ would have to be done numerically but is unnecessary for the purposes of this paper since ϕ_w can be obtained from Eq.16. Eq.A8 describes the electric field in the sheath and, since the potential must vary monotonically with distance in the sheath, then ϕ' must be negative or zero. Therefore Eq.16 is valid if the right-hand side of Eq.A8 is always positive or zero throughout the sheath.

In the usual derivation of the Bohm sheath criterion an equation similar to (A8) is obtained but with $\Gamma_s = 0$ and $j^-/j^+ = 1$ (eg Eqs.8-8 to 8-10 of Ref.8). It is easily shown that $\phi'^2 > 0$ if $\delta_i > 0.5$ so the Bohm criterion is unlikely to be infringed for a highly supersonic plasma with δ_i much larger than 0.5, even if Γ_s is large.

A. Limitation to Sheath Potential due to Space Charge Saturation of the Emitted Electron Current

The space charge of emitted electrons affects the electric field in the sheath, especially near the wall. The field throughout the sheath may be calculated from Eq.A8 (assuming values of δ_i and j^-/j^+) in the following manner:

First a reasonable value of ϕ_w is chosen so that Γ_s can be obtained from Eq.16; then the values of ϕ_w and Γ_s are used to determine ϕ' for various values of ϕ. A series of curves showing the variation of ϕ' with ϕ is presented in Fig.11 which shows that the electric field increases progressively as the potential, ϕ, approaches that at the wall, ϕ_w. The variation of ϕ' with ϕ for small but finite Γ_s is illustrated in Curve 2. It can be seen that both the electric field at the wall, ϕ_w' and the sheath potential ϕ_w, are

reduced as a result of electron emission but that the characteristics of the sheath away from the wall are not much affected.

As Γ_s increases (Curves 3, 4 and 5) the electric field at the wall, ϕ_w', becomes much weaker until with $\Gamma_s = 5.94$ (Curve 6) it becomes zero. This occurs when $\phi_w = 0.509$, the lowest possible sheath potential for which a stable solution can be obtained. In order to avoid such trial and error computations it is necessary to expand Eq.A8 in a Taylor series

where
$$\phi'^2 = \phi_w'^2 + \theta\phi_1'^2 + O(\theta^2) \ , \qquad \text{(A9)}$$
$$\theta = \phi_w - \phi \ .$$

Making use of the series relationship

$$E(t) = \frac{2}{\sqrt{\pi}} \left[\frac{2}{3} t^{3/2} + \frac{4}{15} t^{5/2} + \frac{8}{105} t^{7/2} + \ldots\right] ,$$

it is found that the first non trivial term in Eq.A9 is the zero order term

$$\phi_w'^2 = 4\delta_i\left[\left(1 + \frac{\phi_w}{\delta_i}\right)^{\frac{1}{2}} - 1\right]$$
$$- 2\left(\frac{j^-}{j^+} + \Gamma_s\right)\left(\pi\delta_i \frac{m_e}{m_i}\right)^{\frac{1}{2}}\left[\exp(\phi_w)\ (1 + \operatorname{erf}\sqrt{\phi_w}) - \frac{2}{\sqrt{\pi}}\sqrt{\phi_w} - 1\right]$$
$$- 4\Gamma_s\sqrt{\frac{m_e}{m_i}\delta_i\phi_w} \ .$$

If Γ_s is eliminated via Eq.16 with $s_i = \infty$ and $F(\infty) = (2\pi)^{-\frac{1}{2}}$, then

$$\phi_w'^2 = 4\delta_i\left[\left(1 + \frac{\phi_w}{\delta_i}\right)^{\frac{1}{2}} - 1\right] - \frac{2}{C_\infty}\frac{j^-}{j^+}\left(G - 2\sqrt{\phi_w} - \sqrt{\pi}\right)$$
$$- \frac{2(G - \sqrt{\pi})}{C_\infty}\ \frac{\left[C_\infty - (j^-/j^+)G\right]}{(G + \phi_w^{-\frac{1}{2}})} \qquad \text{(A10)}$$

where
$$G = G(\phi_w) = \sqrt{\pi}\ (1 + \operatorname{erf}\sqrt{\phi_w})\ \exp\phi_w \qquad \text{(A11)}$$
and
$$C_\infty = (\delta_i m_e/m_i)^{-\frac{1}{2}} \ . \qquad \text{(A12)}$$

Equation A10 describes the electric field at the wall and has been

tested for accuracy by numerical comparison with the data in Fig.11. Equations A10-12 are reproduced in Sect.III.B.1 of the main text as Eqs.17-19 and are discussed both in that Section and in Sect.III.D.

B. Limitation to Sheath Potential due to a Modified Bohm Sheath Criterion

At the plasma boundary of the sheath ϕ is small so it is convenient to expand the right-hand side of Eq.A8 as a series in ϕ. By using Eq.16 and the expression

$$E(\phi_w) - E(\phi_w - \phi) = \phi\left[\exp(\phi_w)\ \mathrm{erf}\ \sqrt{\phi_w}\right] - (\phi^2/2)\left[(\pi\phi_w)^{-\frac{1}{2}} + \exp(\phi_w)\ \mathrm{erf}\ \sqrt{\phi_w}\right] + O(\phi^3),$$

it can be shown that the first non-zero coefficient in the series expansion of Eq.A8 is of second order in ϕ so

$$\phi'^2 = \left\{\left(1 - \frac{1}{2\delta_i}\right) - \Gamma_s\left(\frac{\delta_i}{\phi_w}\frac{m_e}{m_i}\right)^{\frac{1}{2}}\left[\frac{1}{2\phi_w} - \frac{j^-/j^+}{\Gamma_s}\right]\right\}\phi^2 + O(\phi^3)\ . \qquad (A13)$$

This expression for the electric field at the plasma boundary of the sheath is reproduced in Sect.III.B.2 of the main text as Eq.20 and is used to derive the modified Bohm criterion (Eqs.21,22) which is discussed in that section and in Sec.III.D.

[1] P J Harbour and M F A Harrison, "The influence of electron emission at the divertor of a tokamak fusion reactor", Paper No.25 in 3rd International Conf. on Plasma Surface Interactions in Controlled Fusion Devices, Culham, April 1978.

[2] P J Harbour and M F A Harrison, "Some consequences of collisionless exhaust flow to the divertor target of a fusion reactor", Paper submitted to IAEA 7th International Conf. on Plasma Physics and Controlled Nuclear Fusion Research, Innsbruck, August 1978.

[3] D Bohm, "Characteristics of Electrical Discharges in Magnetic Fields", p.77 (A Guthrie and R K Wakerling, eds), McGraw Hill, 1949.

[4] G D Hobbs and J A Wesson, Culham Laboratory Report CLM-R61 (1966).

[5] G D Hobbs and J A Wesson, Plasma Physics, 9, 85-87 (1967).

[6] S A Schaaf and P L Chambré, "Flow of Rarefied Gases", Princeton Aeronautical Paperbacks, No.8 (Princeton University Press, 1961).

[7] A E Robson and P C Thonemann, Proc.Phys.Soc., 73, 508 (1959).

[8] F F Chen, "Introduction to Plasma Physics" (Plenum Press, 1974).

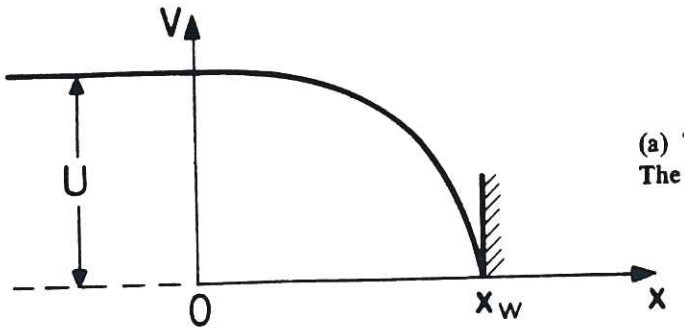

(a) The potential, V, plotted as a function of distance, x. The potential in the plasma, U, is assumed constant.

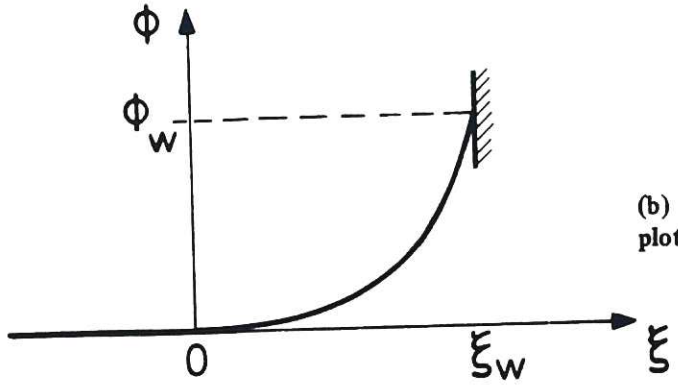

(b) The non-dimensional potential, $\phi = e(U-V)/kT_e$, plotted against the non-dimensional distance, $\xi = x/\lambda_D$.

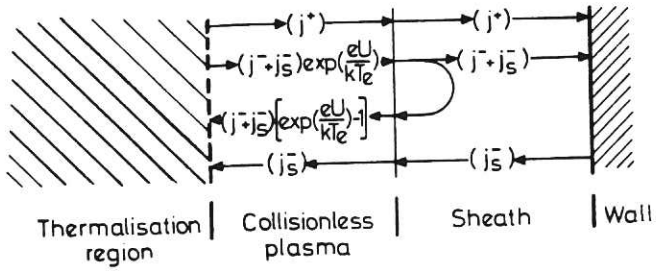

(c) The distribution of current density. If the plasma is at floating potential with respect to the wall, then $j^+ = j^-$. Backscatter of ions and electrons at the wall has been neglected.

Fig.1 The distribution of potential and current density in the plasma and sheath.

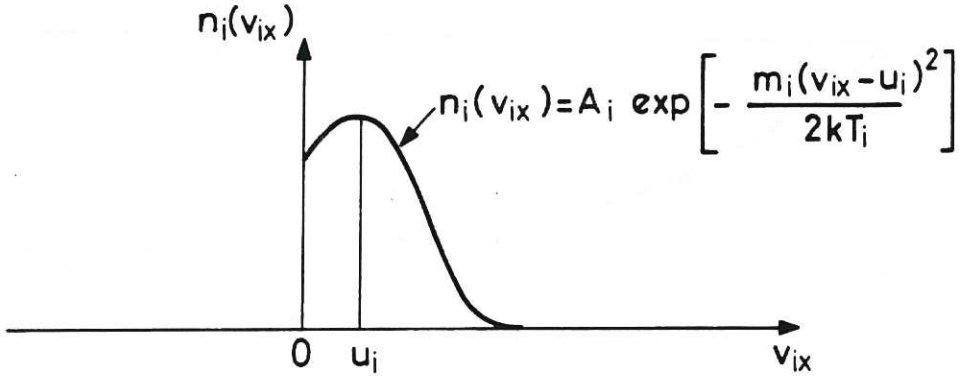

(a) The ion distribution function in the collisionless plasma. In the sheath it is assumed for simplicity that the ion speed ratio, $s_i \to \infty$, where $s_i = (m_i u_i^2 / 2kT_i)^{1/2}$, but this assumption is required only to obtain the limits to the stable sheath region via the Poisson equation.

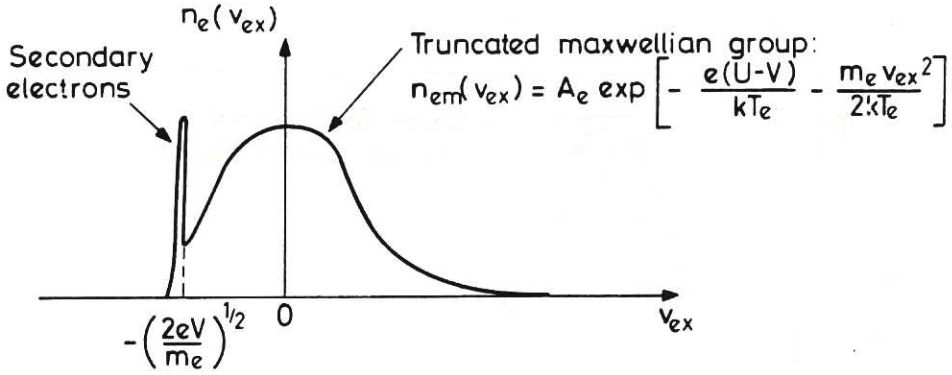

(b) The electron distribution assumed both in the plasma and in the sheath. It is Maxwellian in the y and z directions, while in the x direction it consists of a truncated Maxwellian plus a delta function due to secondary electrons.

Fig.2 The velocity distribution functions assumed in the model.

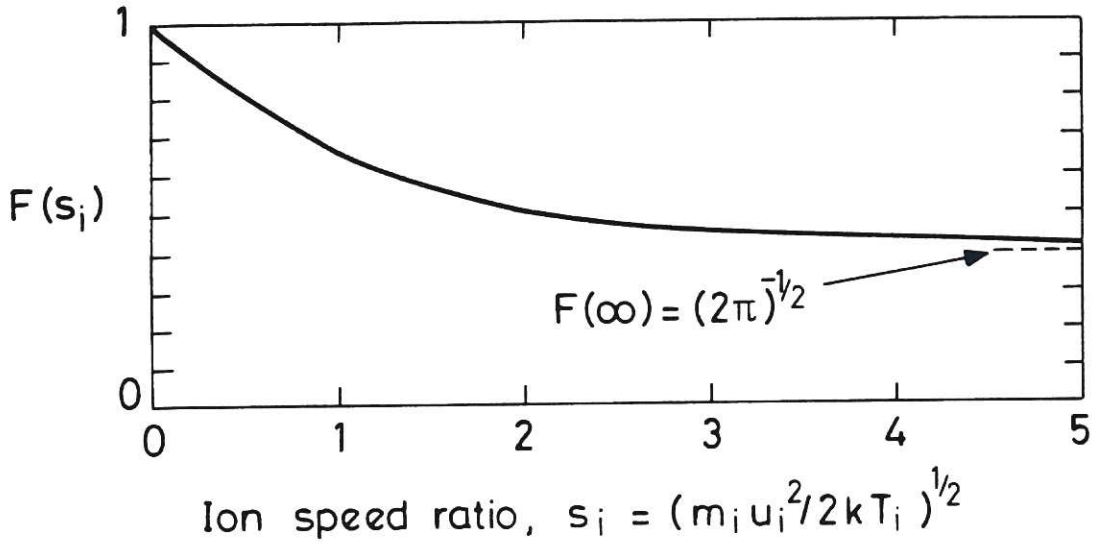

Fig.3 Variation of the function $F(s_i)$ with the ion speed ratio, s_i, as defined in Eq.14.

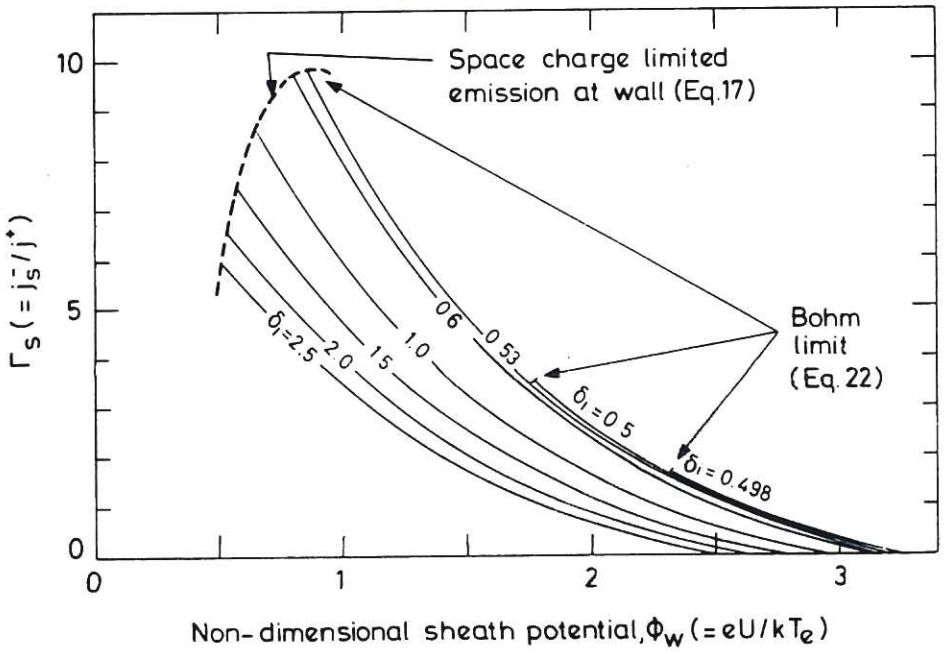

Fig.4 Variation of the effective coefficient for secondary electron emission, Γ_s, with non-dimensional sheath potential, ϕ_w, for various values of the ion energy transport coefficient, δ_i. The evaluation was carried out for a deuterium/tritium plasma sheath (m_i = 2.5amu) at floating potential ($j^+ = j^-$) and with monoenergetic incident ions.

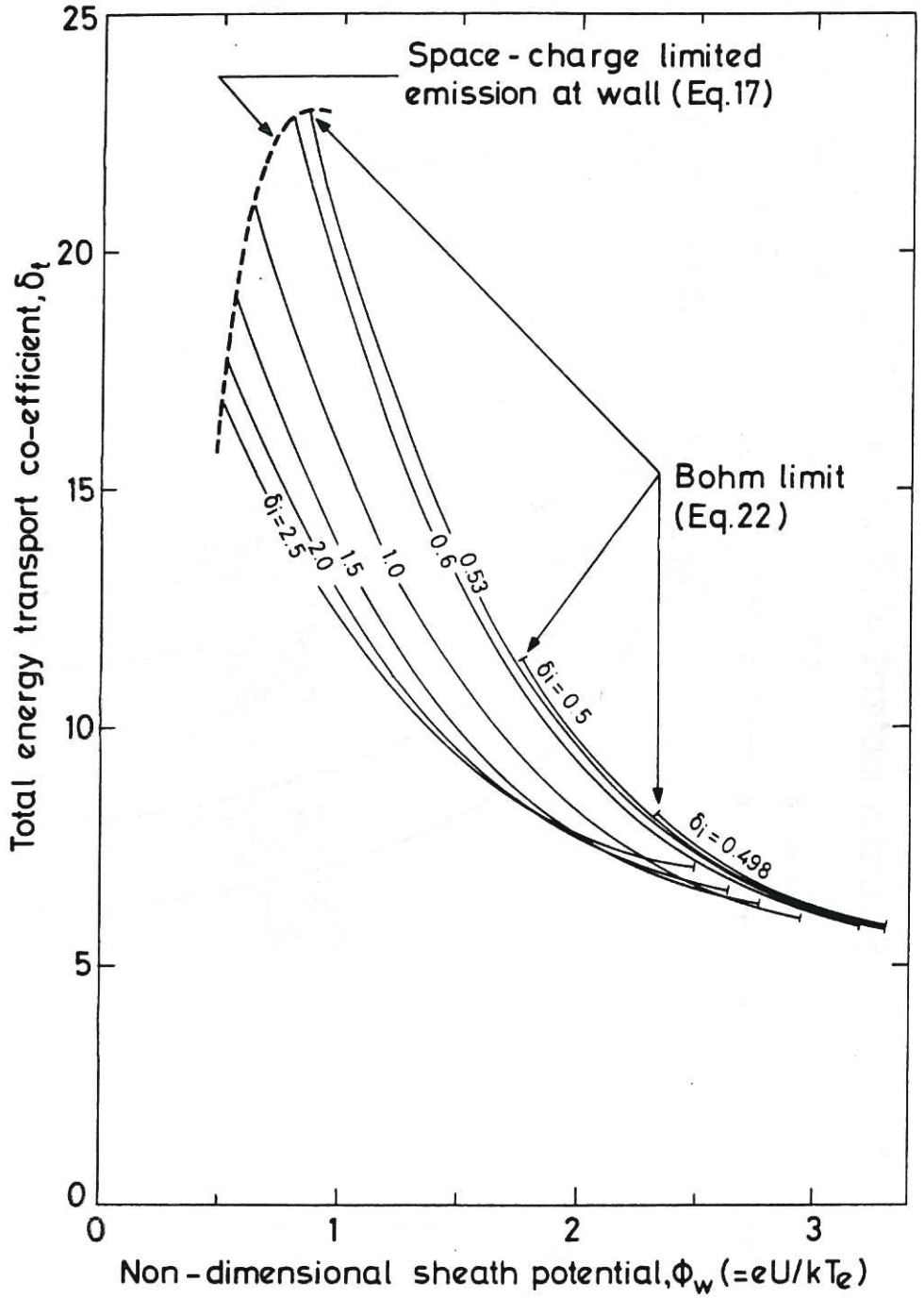

Fig.5 Variation of the total energy transport coefficient, δ_t (Eq.23) with non-dimensional sheath potential, ϕ_w. The plasma is a D–T mixture with the same conditions as in Fig.4.

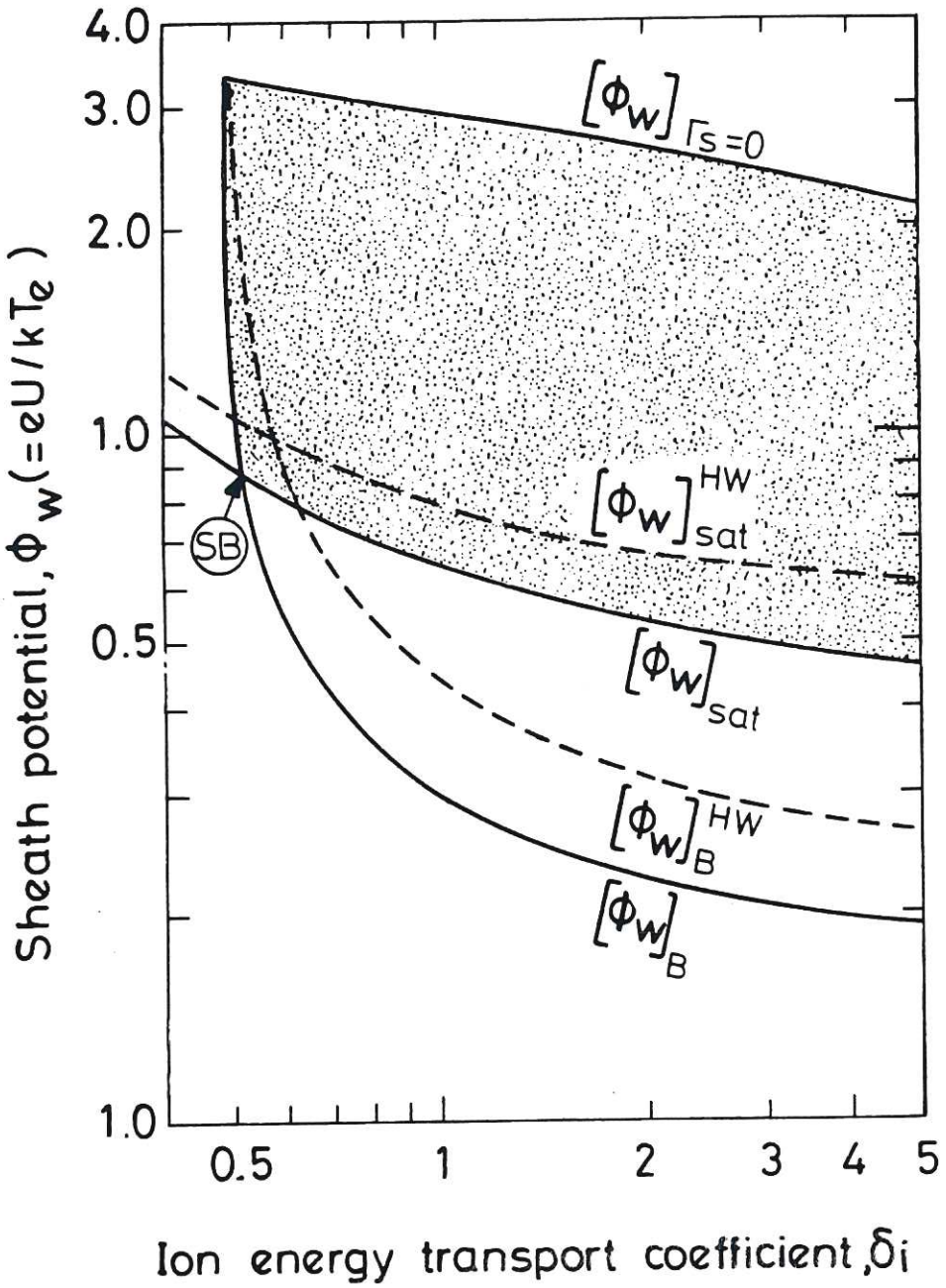

Fig.6 Bounds to the floating sheath potential versus the ion energy transport coefficient. The plasma is a deuterium/tritium mixture (m_i = 2.5amu) with monoenergetic incident ions ($s_i \rightarrow \infty$). The hatched area between $[\phi_w]_{\Gamma_s = 0}$, $[\phi_w]_{sat}$ and $[\phi_w]_B$ defines the regime of a stable sheath based on the present analysis, whereas that between $[\phi_w]_{\Gamma_s=0}$, $[\phi_w]^{HW}_{sat}$ and $[\phi_w]^{HW}_{B}$ is a corresponding regime following the arguments of Hobbs and Wesson. These parameters are described in the text.

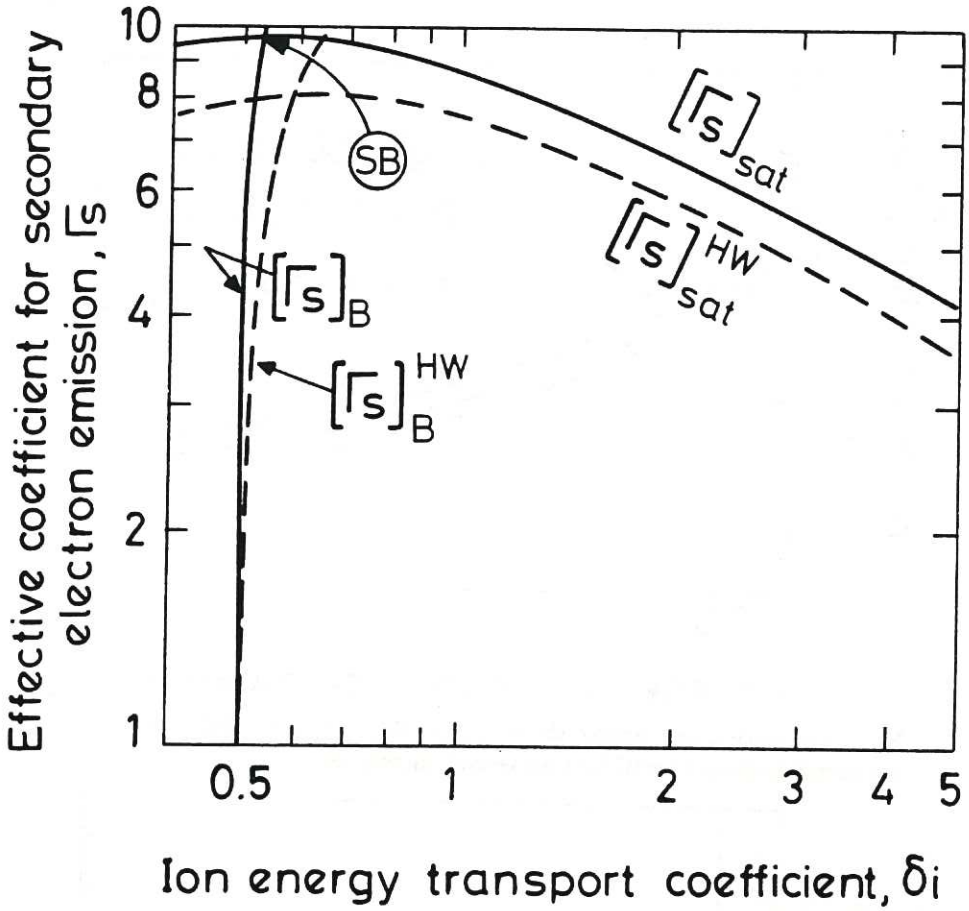

Fig.7 Maximum permitted values of the effective coefficient of secondary electron emission versus ion energy transport coefficient. The curves correspond to similarly labelled curves in Fig.6 and are related to them via Eq.16.

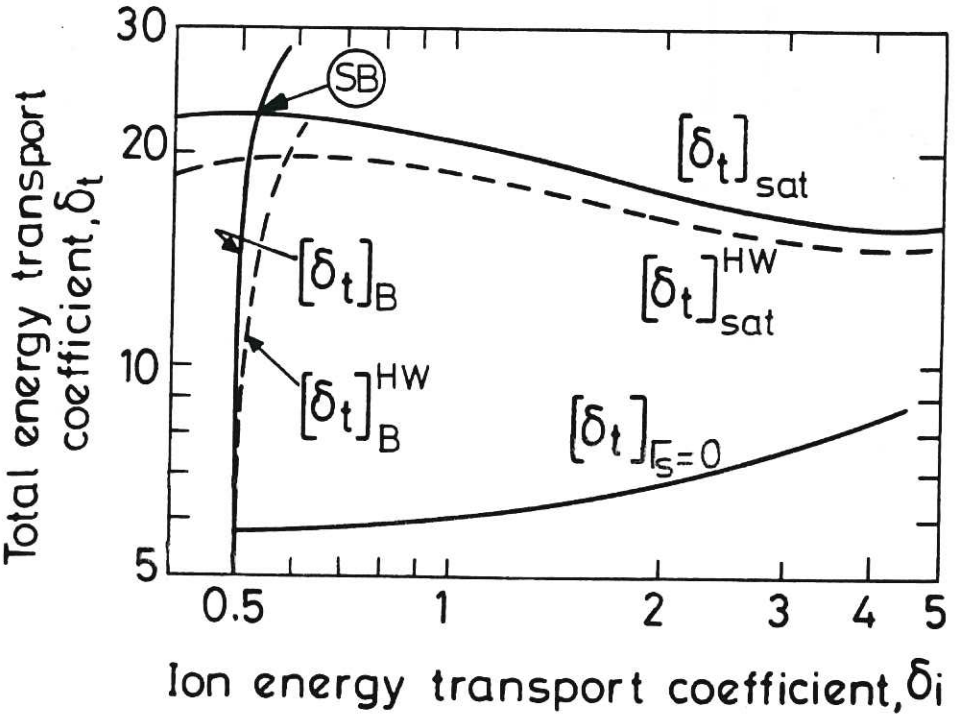

Fig.8 Maximum permitted values of the total energy transport coefficient versus the ion energy transport coefficient. The parameters correspond to those in Figs.6 and 7.

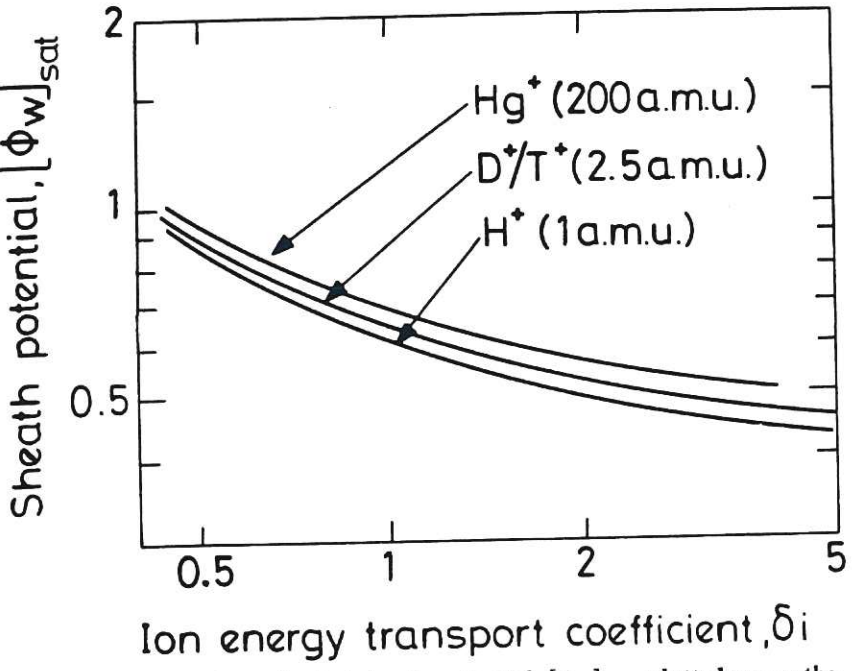

Fig.9 The space charge limited sheath potential, $[\phi_w]_{sat}$, plotted versus the ion energy transport coefficient for several ion masses.

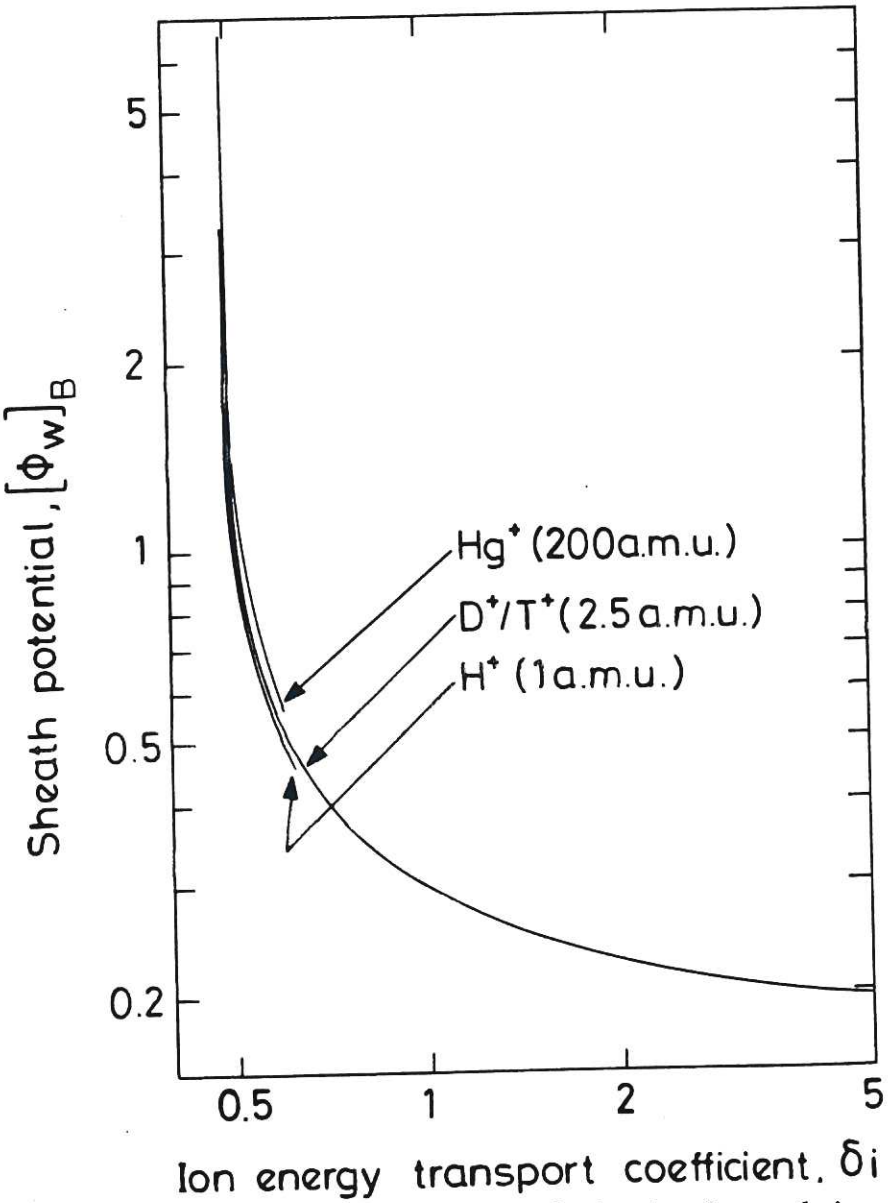

Fig.10 The Bohm limit to sheath potential, $[\phi_w]_B$, plotted versus the ion energy transport coefficient for several ion masses.

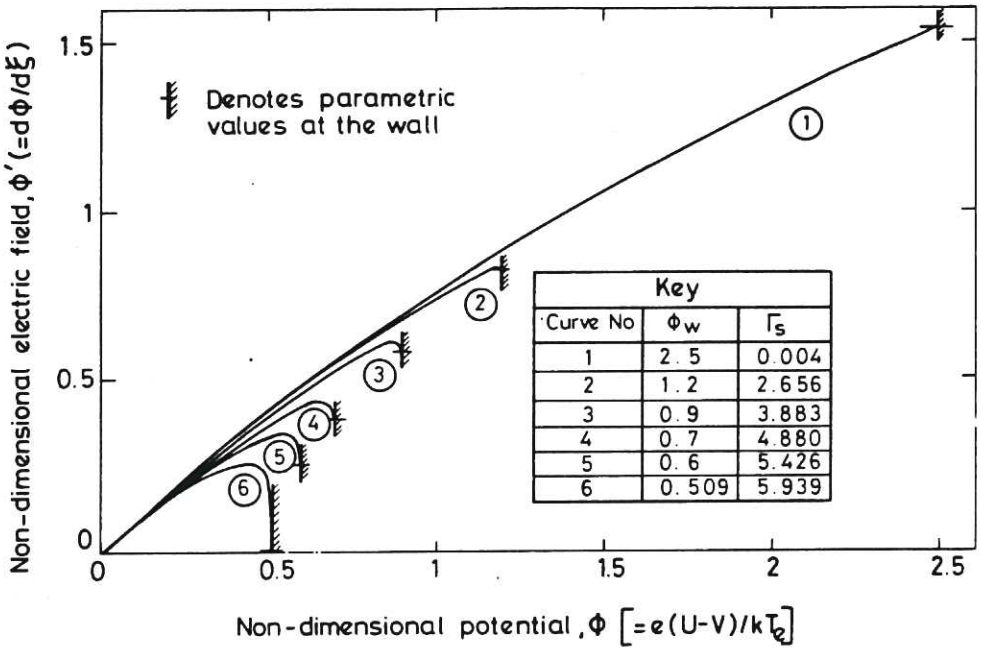

Fig.11 Variation of electric field with potential in a deuterium/tritium plasma sheath (m_i = 2.5amu) at floating potential ($j^+ = j^-$). The incident ions are monoenergetic ($s_i \to \infty$) with an energy characterised by δ_i = 2.5. ϕ' has been obtained from Eq.A8 with ϕ_w as the independent variable and Γ_s from Eq.16.